Heterogeneous Spectrum Bands Aggregation Prototype with Cognitive Radio Capabilities

Emmanouil A. Antonopoulos*†, Fotis Plessas*†, Fotis Foukalas*, Ioannis Zographopoulos†
*Industrial Systems Institute, Athena Research and Innovation Center, Patras, Greece
† Department of Electrical and Computer Engineering, University of Thessaly, Volos, Greece

Abstract—This paper presents the design and simulation of an RF prototype that can provide dynamic carrier aggregation (CA) in future cognitive heterogeneous cellular networks including also access to heterogeneous technologies. To this end, the proposed RF prototype can support heterogeneous multi-band CA scenarios with up to 3-band CA including unlicensed bands. Among other features, cognitive radio capabilities are incorporated to this prototype like spectrum sensing using energy detectors and dynamic CA using switches among the RF chains. The proposed architecture is evaluated in this paper highlighting useful insights of the proposed design. Our future work is to develop the proposed architecture using particular hardware components as an implementation within the framework of SOLDER FP7 project.

Keywords: RF prototype, carrier aggregation, cognitive radio, heterogeneous dispersed bands.

I. INTRODUCTION

Next generation wireless communication systems demands as much as possible the highest data rates. Towards this end, significant techniques have been proposed in the past like MIMO for multi-antenna implementation and recently, like Carrier Aggregation (CA) with multi component carriers (CCs) aggregation. CA provides extended bandwidth by aggregating up to five component carriers (CCs), wherein each CC could be with bandwidth from 5-20 MHz. Maximum of 5 CCs initially proposed and thereby, an amount of 100 MHz aggregated total bandwidth is provided. There are three types of CA as discussed in [1] relying on contiguous or non-contiguous concept, and on inter-band or intra-band CA.

Nowadays, most spectrum is either occupied or fragmented, which leads to the consumption that the third CA scenario (Inter-band Non-Contiguous CA) is the key scenario until new spectrum becomes available. We focus on the following application scenarios: a) aggregation of carriers within FDD bands, b) aggregation of carriers of licensed and unlicensed spectrum, and c) aggregation of carriers of FDD and TDD bands. Apart from the extension of bandwidth, it is vital for beyond 4G to provide cognitive capabilities such as dynamic CA provision and spectrum sensing in order to opportunistically exploit spectrum.

There are several techniques in order to implement spectrum sensing. Due to its simplicity and no requirement on a priori knowledge of primary user signal, energy detection (ED) is the most popular sensing technique. ED can be implemented both as a non cooperative and cooperative scheme between primary and secondary users. Without cooperation between the primary users (PUs) and the secondary users (SUs), SUs monitor the licensed frequency band and opportunistically transmit when they detect idle of PUs [2]. The second option called cooperative spectrum sensing, occurs when a group of cognitive radios (CR) share the sensing information they have obtained in order to boost the efficiency of spectrum usage over the area. Moreover, this approach gives the opportunity to secondary users to not only exploit licensed frequency band in the absence of PUs but also exploit spectrum holes in the frequency band even when a PU is active [3].

To the best of our knowledge, there are no significant works on the RF prototype for a multi-band receiver and transceiver for CA in a dynamic fashion exploiting the advances in cognitive radio technology. To be specific, as illustrated in [4], a carrier-aggregated modulator with two CCs in the transmitting path is proposed. This architecture uses four I/Q modulators, wherein each one of them consist of a current mode logic divider and two Gillbert-cell mixers. The proposed modulator has three switching states which are determined by the ON/OFF states of the four modulators used. In [1], an overview of design challenges of CA-capable terminals is presented. Different radio architectures are discussed from the perspective of design trade-off. A "scalable" block downconversion receiver architecture that can support multiple carriers while providing an Image Rejection Ratio (IRR) greater than 70 dB with the use of a new broadband low noise amplifier (LNA) is proposed in [5]. Finally, in [6], a 0.1-6.0 GHz dual-path SDR transmitter supporting intra-band carrier aggregation has been implemented in 65-nm CMOS.

Compared to the previously reported works, the proposed architecture differentiates as follows: (i) it provides inter-band contiguous and non-contiguous intra-band CA with the capability to receive and transmit up to three carriers simultaneously, (ii) it provides both time-division duplex (TDD) and frequency-division duplex (FDD) modes, (iii) it demonstrates CA between licensed and unlicensed bands, (iv) it demonstrates MIMO capabilities and finally, (v) it employs energy detection for spectrum sensing. We use commercial discrete components to build the demo prototype, which provides the aforementioned cognitive radio functionalities.

The reminder of this paper is organized as follows. Section II describes the proposed architecture. Section III presents the dynamic CA features with cognitive radio capabilities. Section IV reports the simulation results. Section V describes the performance evaluation. Finally, Section VI presents the conclusions and describes future work in this topic within the

framework of the SOLDER FP7 project [7].

II. RF PROTOTYPE ARCHITECTURE

Fig.1 presents the full architecture of the proposed RF prototype. The TX/RX chains consist of five fully integrated transceivers, which are used in order to drive the signals from the baseband to the RF part of the platform. The second building block shapes the RF Front End (RFFE), and is the part of the prototype that allows selecting one specific band and duplexing scheme. Includes duplexers and low noise amplifiers for RX paths and duplexers, power amplifiers (PA) and filters for the TX paths. The third building block consists of switches and power combiners/splitters for both the licensed and unlicensed spectrum aggregation. For enhanced CA and MIMO investigations like single/dual/triple antenna CA aggregation and MIMO cases, additional switching and combiner stages are necessary. Moreover, power detectors are used in order to measure the power levels at the channel, which is essential for the implementation of both spectrum sensing and dynamic CA.

The proposed prototype is capable of using either one antenna per CC or one antenna for all CCs allowing thereby the antenna diversity or multiplexing respectively. As far as inter-band CA with MIMO multiplexing is concerned, the standard implementation is to use one antenna for all CC. In order to provide multiplexing with MIMO, then one antenna will be used for the transmission of all CCs; however, this implementation depends on the frequency range of the carriers as seen in [1]. The proposed prototype can implement both types of transmission. In order to achieve equivalent power levels for the transmission process for both schemes, we placed attenuators at the RFFE and adjusted the power combiners for both intra-band and inter-band CA.

Using the configurable RX/TX chains the transmitter operates in LTE band 3 (1710-1785 MHz/1805-1880 MHz), in LTE band 7 (2500-2570 MHz/2620-2690 MHz), in LTE band 20 (832-862 MHz/791-821 MHz) and in LTE band 38 (2570-2620 MHz), and in the ISM band (5150-5350 MHz). Multiple frequency synthesizers are locked to a common reference to achieve RF carrier synchronization in the MIMO RX and TX chains.

III. DYNAMIC CARRIER AGGREGATION WITH COGNITIVE RADIO CAPABILITIES

A. Multi-band CA

The proposed prototype is capable of performing both intra-band and inter-band CA using up to three CCs. In intra-band CA, all CCs are included in the same frequency band while in inter-band CA, CCs belong to different frequency bands. Moreover, the prototype can support aggregation between FDD or/and TDD or/and unlicensed bands.

B. Band Switching

The prototype has the ability to dynamically decide about the number of CCs for both the Inter-band and the Intra-band
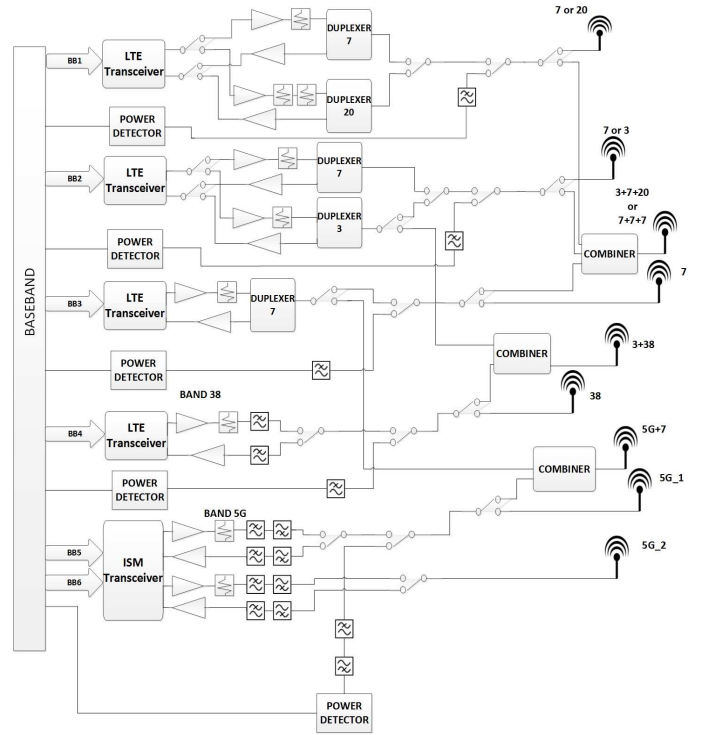

Fig. 1: RF prototype Architecture

CA scenarios.The same technique is used for both use cases regarding the decision about the number of CC which will be used for the CA scenarios.On both use cases, the decision regarding the number of CC's depends: (i) on the coverage area of the receiver, (ii) on the availability of the spectrum in this bands and (iii) the power levels of the CC which were received earlier in the channels of interest. More particularly, we have to transmit the CC's in LTE bands which are within the coverage are of the receiver, so that the the receiver can receive all the carrier components. Secondly, prior to the transmission, all the channels which will be used, have to be idle in order to be used from the transmitter for the transmission of all CC's. Taking in to account the aforementioned limitations, when the received CC have high levels of power, then a maximum of three CC's will be used for CA at the transmission. While when the received CC are poor in terms of power, then fewer CC's will be used for the transmission. The activity of the channels can be detected by using the spectrum sensing technique which is described in the subsection below. The feedback obtained by the aforementioned technique is used as input to a complex algorithm, in order for the algorithm to decide about the number of component carriers.

C. Spectrum Sensing

The proposed prototype also incorporates spectrum sensing in order to opportunistically access licensed spectrum. By using four paths where each path is set to a certain frequency band, the prototype is able to detect whether a transmission

TABLE I: 3GPP Use Cases

Antennas used for TX	Antennas used for RX	CA scenario	Bands
3	3	MIMO Diversity	3, 7, 20
1	1	Inter-band 3-band CA	3, 7, 20
1	1	Intra-band CA	7

TABLE II: HW Components

Part name	Quantity	Description
AH323-G	6	Driver Amplifier
HMC392LC4	2	LNA Amplifier
TGA2599-SM	2	Driver Amplifier
TQP3M9038	6	LNA Amplifier
885043	3	Band pass filter (Band 38)
TQM976027	4	Duplexer (Band 7)
TQQ1003	2	Duplexer (Band 3)
856979	2	Duplexer(Band 20)
LT5538	4	Power Detector
LTC5533	1	Power Detector
GP2Y+	1	Power Splitter/Combiner
SC4PS-33+	1	Power Splitter/Combiner
EP2C+	1	Power Splitter/Combiner
MASW-007588	42	Switches
PE43502MLI	14	Attenuators
LFCN-5850+	2	Low Pass Filter
HFCN-4400D+	2	High Pass Filter

is already in progress. Each path contains one band-pass filter and a power detector. The prototype periodically scans the channel and sends the data to the baseband, when the transceiver is set for a transmission and the channel is free, the transmission starts. The prototype uses RF power detectors, which consist of cascaded amplifiers and RF detectors. The output currents from every RF detector are combined and low-pass filtered before applied to the output buffer amplifier. As a result, the final DC output voltage approximates the logarithm of the amplitude of the input signal. Thus, when the baseband receives the feedback regarding the output voltage by using an adaptive algorithm, it can identify whether a signal is active in the channel or not.

IV. SIMULATION RESULTS

In this section, we provide the simulation results obtained using the following 3GPP parameters, listed in Table I above [8].

The different use cases have been simulated using Keysight's Advanced Design System 2013 EDA software. The proposed architecture was designed assuming hardware discrete components. More specifically, regarding the TX&RX chains, the architecture uses four LMS6002D [9] integrated chips for the licensed spectrum and one AD9361 [10] chip, which is a second generation transceiver with MIMO capabilities for the unlicensed spectrum. Both the LMS6002D and the AD9361 are provided with tunable channel bandwidth of more than 20 MHz and can support both TDD and FDD operation. Both transceivers incorporate a multiplicity of RF inputs and outputs to enable a wide range of features to be implemented. The full list of the components used is presented in Table II.

Frequency domain Harmonic Balance (HB) simulation has been carried out to analyse both the MIMO Diversity and the Inter-band CA scenario. This method is ideal in order to study the system's performance in terms of power and harmonic frequencies of the sub-systems. A Line-of-Sight (LoS) link is assumed to simulate the channel impairments. This option introduces the losses of free space depending on the distance and the center frequency, which set by the user. Moreover, the bandwidth and the gain of both the transmitters and receivers antennas can be specified by the user. The LoS path length was set to 1km between the transmitter and the receiver. Moreover the maximum output power was trimmed to be below 23 dBm in order to be compliant with the 3GPP specifications [11]. For both HB simulations, three CCs were used with center frequencies of 845 MHz, 1768 MHz and 2537 MHz respectively. The first use case assume that each CC was transmitted and received by different antennas,

using three antennas respectively. For the second use case, we assumed one antenna for transmission and one for the reception of all carrier components. The first use case is provided for the antenna diversity and the second used for antenna multiplexing.

Figure 2 depicts the power levels of the CCs before the transmission when using one antenna for the transmission. The first CC shows a power of 21.497 dBm, the second CC shows a power equivalent to 21.493 dBm and the third one equal to 21.495 dBm. In Fig.3, the power levels of the received signals at the receiver's antenna are depicted when using one antenna for the reception. The power levels after the reception for all three CCs are -49.565 dBm for the first CC, -55.851 dBm for the second CC and -58.956 dBm for the third CC respectively.

Figure 4 and Fig.5 depict the simulation results for the transmission and reception in terms of power for the second use case. As expected the differences in terms of power for the two schemes were negligible. Figure 4 depicts the power levels of the CCs right before the transmission when using three antennas for the transmission. The first CC has a power of 21.501 dBm, the second CC has a power equivalent to 21.495 dBm and the third one equal to 21.498 dBm. Simulation results in terms of power after the reception of the CCs when using three antennas can be seen in Fig.5. The power levels after the reception for all three CCs are -49.562 dBm for the first CC, -55.852 dBm for the second CC and -58.970 dBm for the third CC respectively. Three different colors have been used,where each one represents the Tx/Rx of a CC from a different antenna. Both figures also depicted the harmonics of the other CC can be seen.

Moreover, we studied the effect of the pathloss between the transmitter and the receiver by tuning the distance between the transmitter and the receiver from 0.5 km to 3 km. Due to space limitation, we will only give the maximum and the minimum power levels for each CC and omit the figures. The difference on power levels is observed regarding the reception of the three CCs for both schemes. For the first CC the power levels regarding the reception had a variation from -43.5 dBm to -59.1 dBm, for the second CC from -49.8 dBm to -65.4 dBm, while for the third CC the power levels varied between
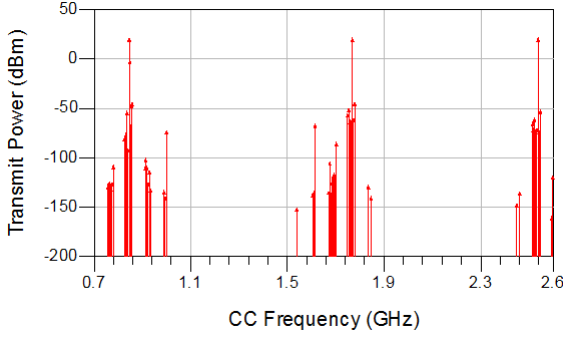
-52.9 dBm to -68.5 dBm.

Fig. 2: Transmit power using 1 antenna versus CC frequency for f_{c1} = 845 MHz, f_{c2} = 1768 MHz and f_{c3} = 2537 MHz
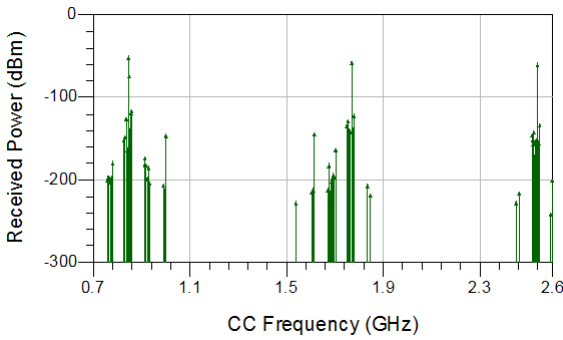

Fig. 3: Received power using 1 antenna versus CC frequency for f_{c1} = 845 MHz f_{c2} = 1768 MHz and f_{c3} = 2537 MHz
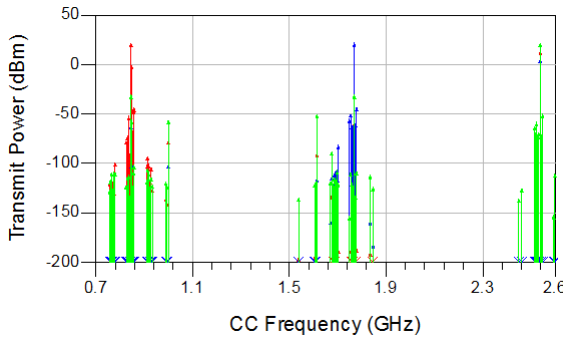

Fig. 4: Transmit power using 3 antenna versus CC frequency for f_{c1} = 845 MHz, f_{c2} = 1768 MHz and f_{c3} = 2537 MHz

Digital signal processing (DSP) simulations were carried out to analyse the intra-band CA scenario. In this way, we can demonstrate some of the transmitter characteristics such as the TX and RX spectrum waveforms. The simulation setup is identical to that used for the HB simulations. The frequency distance between the center frequencies of the CC, which are used for the intra-Band CA has to be an integral multiple of 300 kHz. Given this limitation, three CCs with center frequencies of 2515 MHz, 2535.1 MHz and 2555.2 MHz were chosen and each of them had a bandwidth of 20 MHz with QPSK modulation. After the aggregation in LTE band 7, a
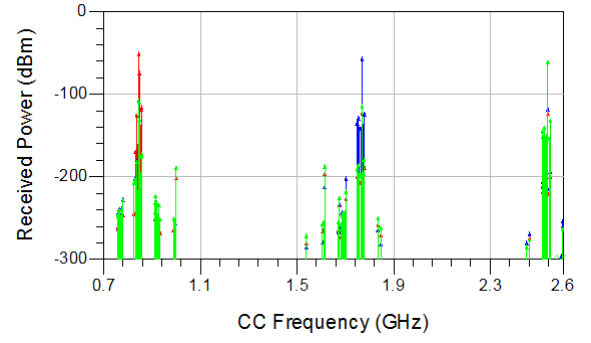

Fig. 5: Received power using 3 antennas versus CC frequency for f_{c1} = 845 MHz, f_{c2} = 1768 MHz and f_{c3} = 2537 MHz
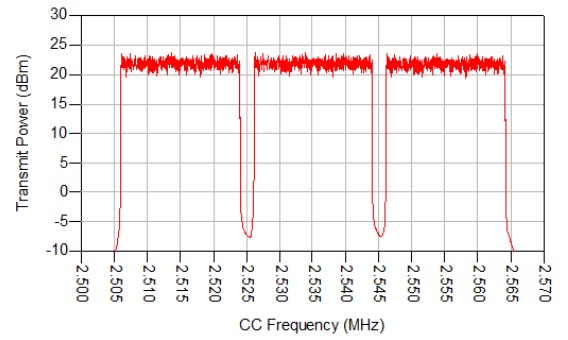

Fig. 6: Spectrum of Intra-band CA scenario with three CCs

total of 60 MHz bandwidth was achieved. Figure 6 depicts the spectrum of the CC after the aggregation, where the power levels for the three CCs are 21.418, 21.417 and 21.412 dBm respectively. Fig.7 depicts the spectrum of the received signal at baseband frequency for one of the three CCs.

Table III, depicts simulation results for the voltage levels at the output of the power detector regarding the inter-band CA scenario. Finally, for a typical setup, the NF (Noise Figure) is 6.71 dB, and the input referred 1 dB compression point and
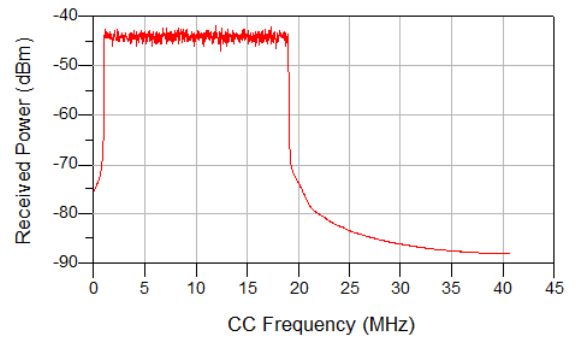

Fig. 7: Spectrum of one CC at the receiver for the Intra-band CA scenario

IP3 are -22.4 dBm and -11.4 dBm respectively.

TABLE III: INPUT AND OUTPUT OF THE POWER DETECTOR

Carrier Frequency (MHz)	Input Power (dBm)	Output Voltage (V)
845	-50.563	0.7
1768	-56.849	0.62
2537	-59.971	0.5

V. PERFORMANCE EVALUATION

For the PHY layer, which consists of a digital baseband part and analog RF part, the digital part is under implementation in a motherboard FPGA while the analog part is under implementation in an RF daughterboard (Fig.8). The Xilinx Zynq-7000 SoC ZC706 evaluation kit, including hard-IP dual ARM Cortex-A9 core processor will be used providing computational power for possible extensions of the platform for upper layers in terms of software. The RF daughterboard includes the following blocks: (i) TX&RX chains, (ii) RF Front End (RFFE) and (iii), Switching and power detection module. High speed connectors have been used for the connection of the daughterboard with the motherboard in order to form a complete platform. On the transmit side, IQ DAC samples from the digital baseband are provided to the LMS6002D/AD9361 on a 12 bit parallel CMOS input level bus. On the receive side, the analog receive IQ signals are converted into the digital domain using the on chip receive ADCs and provided as an output from the LMS6002D/AD9361 to the digital baseband on a 12 bit CMOS output level parallel bus. The functionality of the transceivers is fully controlled by a set of internal registers which can be accessed through a serial port interface. Amplifiers, switches and attenuators are also controlled by the baseband. The hardware components used to develop the RF daughterboard are listed on Table II. Regarding MIMO evaluation, pre-coding at the baseband transmitter and post-coding at the baseband receiver are under development to jointly cancel the interference from/to unlicensed bands. At the RF daughter card all the local oscillators (LOs) in the different radio paths are synchronized using a common reference. The designed platform is currently under fabrication and measured results will be provided in our future work.

VI. CONCLUSIONS AND FUTURE WORK

In this paper, we have presented an RF prototype with cognitive capabilities. The proposed prototype is cognitive radio enabled by implementing multi-band CA, dynamic CA through switching among the bands and spectrum sensing. It can support two schemes regarding the transmission and reception of signals by using one antenna for the transmission of all CCs and one antenna for the reception of all CCs respectively, or using three antennas, where each antenna was assigned to a CC for both transmission and reception. In this way, both multiplexing and diversity baseband algorithms can be bench-marked. Moreover, simulation results regarding the power of the received signals when altering the distance of the base station and the user equipment for both schemes were provided. We also presented simulation results in terms of
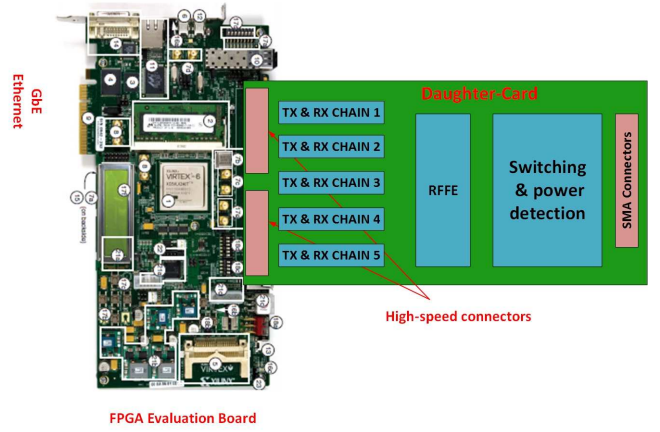

Fig. 8: Block diagram of the overall platform

power for multi-band CA scenarios and made a theoretical approach as far as dynamic CA and spectrum sensing are concerned. Our future work is also described that is the development of this prototype on a daughtercard with discrete chipset components in order to demonstrate dynamic CA capabilities within the framework of the SOLDER FP7 project.

REFERENCES

[1] C.S. Park, L. Sundstrm, A. Walln and A. Khayrallah, Carrier Aggregation for LTE-Advanced: Design Challenges of Terminals, IEEE Communi. Magazine, vol.51, no.12, pp. 76-84, Dec. 2013.
[2] W. Han, J. Li, Z. Tian and Y. Zhang, Dynamic Sensing Strategies for Efficient Spectrum Utilization in Cognitive Radio Networks, IEEE Trans. Wirel. Communi., vol.10, no. 11, Nov. 2011.
[3] A. Ghasemi, E.S. Sousa, Collaborative spectrum sensing for opportunistic access in fading environments,. in Proc. 2005 First IEEE International Symposium on New Frontiers in Dynamic Spectrum Access Networks (DySPAN 2005), Baltimore, USA, pp. 131-136, Nov. 2005.
[4] F-H. Chung, J-Y. Li, C-H. Chi, C-M. Lai, C-H. Tu, P-H. Wu and YJ. Chuang, Design of Carrier-Aggregated Modulator for LTE-Advanced, in Proc. 2014 IEEE MTT-S International Microwave Symposium (IMS), Florida, USA, pp. 1-3, Jun. 2014.
[5] S-C. Hwu and B. Razavi, A Receiver Architecture for Intra-Band Carrier Aggregation, in Proc. 2014 Symposium on VLSI Circuits Digest of Technical Papers, Honolulu, USA, pp. 1-2, June 2014.
[6] Yun Yin, Baoyong Chi, Zhigang Sun, Xinwang Zhang, and Zhihua Wang, A 0.16.0-GHz Dual-Path SDR Transmitter Supporting Intraband Carrier Aggregation in 65-nm CMOS, IEEE Transactions on Very Large Scale Integration (VLSI) Systems, vol. pp, no. 99, June 2014.
[7] F. Kaltenberger, F. Foukalas, O. Holland, Sl. Pietrzyk, S. Thao and G. Vivier, Spectrum overlay through aggregation of heterogeneous dispersed bands, Networks and Communications (EuCNC), 2014 European Conference on, pp. 1-5, Jun. 2014.
[8] 3GPP TR 36-850, Inter-band Carrier Aggregation, Rel.11, v11.2.0, Mar. 2015.
[9] Lime Microsystems, URL: http://www.limemicro.com/download/LMS6002Dr2-DataSheet-1.2r0.pdf
[10] Analog Devices, URL:http://www.analog.com/en/products/rf-microwave/integrated-transceivers-transmitters-receivers/wideband-transceivers-ic/ad9361.html
[11] UE maximum output power, URL:http://www.etsi.org/deliver/etsi_ts/136100_136199/136101/10.01.01_60/ts_136101v100101p.pdf